ELSEVIER

Experimental Thermal and Fluid Science 18 (1999) 334–340

Experimental Thermal and Fluid Science

An experimental investigation of combined turbulent free and forced evaporation

Michael T. Pauken [1]

Department of Mechanical Engineering, Washington University, Campus Box 1185, St. Louis, MO 63130, USA

Received 1 May 1998; received in revised form 17 September 1998; accepted 4 October 1998

Abstract

The wide variation in correlations available in the literature for predicting water evaporation rates in a moving air stream necessitated a new investigation to determine which correlations can be considered reliable. Water evaporation measurements were made from a heated pool (a class-A pan) into a low speed wind tunnel. The evaporation regime examined combined turbulent free and turbulent forced convection over the range $0.1 < Gr_m/Re^2 < 10.0$. The data includes the range in which combined convection modes are important, as well as the limits where either free or forced convection effects may dominate. The data are compared to several evaporation correlations based on laboratory wind tunnel data. These historical correlations do not produce consistent estimates in predicting evaporation rates. It is believed that the apparent inconsistencies arise because many correlations do not adequately describe the appropriate evaporation regimes for which they are valid. A new correlation using the combined free/forced convection Sherwood number has been developed to predict evaporation rates for a moving air stream. This correlation allows the results of this study to be extended to other evaporating conditions (i.e. variation in surface geometry and air turbulence levels) than those described here. For a 95% confidence limit, the Sherwood number correlation matches the data within ±7.9%.

Keywords: Water evaporation; Turbulent convection; Mixed convection; Wind tunnel

1. Introduction

The ubiquitous phenomenon of water evaporation is of interest in a variety of fields such as hydrology, irrigation, oceanography, meteorology, and civil, chemical, industrial, mechanical and nuclear engineering. Consequently, the subject has generated an enormous volume of literature since John Dalton published his treatise on evaporation in 1802 [1]. This wealth of information poses problems for the modern researcher or engineer wanting to find a reliable answer to a simple question such as "how much water will evaporate from a given body of water under certain conditions?". Correlations for evaporation into still air can be found in most textbooks on heat and mass transfer. However, when the air stream is moving over a water surface, these correlations do not exist, except for Dr. Carrier's correlation used by the ASHRAE Fundamentals handbook. Unfortunately, most practicing engineers familiar with this equation know it tends to overpredict actual evaporation rates. Other correlations in the literature do not correlate well with each other. Thus, the author felt it necessary to investigate water evaporation into a moving air stream.

The present study of evaporation has been motivated by the need to determine evaporative water losses from a nuclear spent-fuel disassembly basin. The fuel rods are temporarily stored in these basins and cut to short lengths in preparation for long-term storage and disposal. A typical disassembly basin absorbs residual decay heat from the fuel rods, which creates a thermally loaded body of water. Accurate estimates of the evaporation rate assist in determining whether an aging disassembly basin experiences leakage. The basin building has a high air turnover rate to keep airborne tritium levels low. Consequently, there is a small but significant forced convection over the water surface of the basin and still air evaporation correlations are not applicable to the basin environment.

Water evaporation occurs under several different conditions, which may be categorized according to the

[1] Tel.: 1 314 935 6077; fax: 1 314 935 4014; e-mail: mtp@mecf.wustl.edu

0894-1777/99/$ – see front matter
PII: S0894-1777(98)10038-9

flow regime of the system. A general description of evaporation regimes would identify laminar and turbulent conditions for both the free and forced convection mechanisms. Thus, there are six possible combinations of the convection elements:

- Laminar free convection only,
- Laminar free convection with laminar forced convection,
- Laminar free convection with turbulent forced convection,
- Turbulent free convection only,
- Turbulent free convection with laminar forced convection,
- Turbulent free convection with turbulent forced convection.

Laminar free mass convection occurs when the dimensionless product $Gr_mSc < 2 \times 10^7$. These conditions only occur when the water is unheated and the air temperature is near the water temperature. Sparrow et al. [2] have investigated the case of laminar free convection without a forced convection component. Such conditions are found primarily in indoor environments. In an outdoor environment, such conditions are not found to last for long periods in nature since water bodies and the surrounding atmosphere experience frequent and significant temperature differences.

Turbulent free mass convection occurs with warm water bodies in which the temperature- and concentration-related buoyancies assist each other in creating an upward movement of vapor from the water surface. Boelter et al. [3] and Pauken et al. [4], among many others, have investigated cases of turbulent free convection in still air. These conditions frequently occur in thermally loaded (i.e. heated) water bodies such as power plant cooling ponds or fuel rod disassembly basins.

Forced mass convection under natural atmospheric conditions is difficult to characterize as being laminar or turbulent, based only upon the Reynolds number. In general, it can be said that atmospheric wind conditions tend to be turbulent because of the roughness of the surface.

Indoor conditions may often be laminar, depending on the nature of the air conditioning system servicing the space occupied by the water surface. Turbulent conditions can easily be generated by air blowing across the water surface of a pool. The majority of wind tunnel-based laboratory measurements of evaporation take place with a turbulent air stream either by design or by default. Investigators who have worked with turbulent flow include: Rohwer [5], Carrier [6], Hinchley and Himus [7], Powell [8] and Farley [9]. Few cases of laminar forced convection appear in the literature. The most notable work is that of Albertson [10].

2. Experimental apparatus and procedure

The most noteworthy features of this investigation are the large size of the evaporation pan and the low velocity (0.33–1.45 m/s) of the air stream used in these experiments. All of the previous investigations found in the open literature making evaporation measurements in wind tunnels used small evaporation pans – ranging in size from petri dishes to circular pans around 30 cm in diameter. Furthermore, most investigations examined evaporation under much higher air velocities (e.g. 1–10 m/s) which may diminish the influence of free convection.

It is well known that the size of the pan influences the evaporation rate due to convective edge effects. Small pans have a greater portion of their interior surface affected by convection due to density gradients around the pan edges. Consequently, some evaporation models take into account the surface area in their predictions.

Although the Reynolds numbers encountered in these experiments are of the same order of magnitude as of many previous investigators, the distinction here is that we used a large diameter tank with low air velocities. The purpose of this was to examine the effect on evaporation in which both free and forced convection modes are present on the same order of magnitude. Experiments with small pans and high air velocities examine evaporation with forced convection strongly dominating free convection.

A brief description of the experimental apparatus follows. A more detailed description may be found in Pauken et al. [11]. The evaporation tank used in this investigation is the size of a standard class-A pan developed for meteorological observations. The inside diameter of the pan is 1.18 ± 0.01 m. The essential features of the experimental apparatus are shown in Fig. 1.

The evaporation tank was 30 cm deep and had an electric heater located at the bottom to maintain the water at elevated temperatures. The heater was regulated by a PID controller. The tank was insulated around the sides and the bottom to reduce heat loss. The water temperature was measured by a series of thermocouples located just under the water surface. The water temperatures used in this investigation ranged from 25°C to 50°C in approximately 2.5°C increments.

The water mass loss in the evaporation pan was determined by connecting it to a smaller pan that rested on an electronic scale through a siphon tube. Thus, the water loss in the evaporation tank was proportional to the mass change in the small weighing pan. The proportional constant was determined by removing a

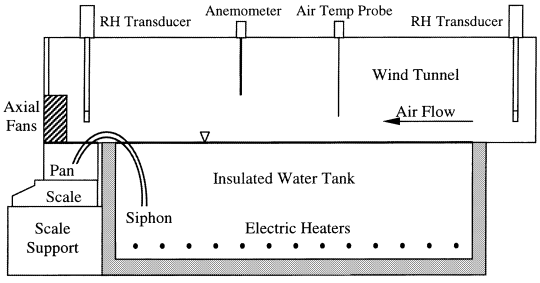

Fig. 1. Schematic representation of water evaporation apparatus.

measured mass of water from the water tank and recording the change in mass on the scale. Thirty-seven observations using this technique were made at various water levels in the tank. It was found that an average of 41.51 ± 0.65 g (95% confidence interval) of water was removed from the water tank for a 1-g change on the scale. When the water temperature of the evaporating surface was different from the weighing pan temperature, a correction for the density difference was made. The scale had a 3-kg capacity with 1-g resolution. Data from the scale was read by a personal computer data acquisition system every 10 min during each experimental run.

A low speed wind tunnel was attached to the upper edge of the evaporation tank. The air was drawn through the wind tunnel by a row of twelve axial fans. A series of baffles were placed in the upstream end of the wind tunnel to create a turbulent velocity field and to ensure a uniform air movement over the evaporation surface. The thermodynamic conditions of the air were determined by a pair of relative humidity transducers located at the inlet and outlet of the wind tunnel. The transducers were found to measure relative humidity within ±2% of known values over four different saturated salt solutions. The air temperature was measured by a thermocouple located over the mid-point of the evaporation pan. All thermocouples were calibrated at three temperatures in a circulating constant temperature bath with an NIST traceable thermometer. The accuracy of the T-type thermocouples was determined to be ±0.2°C when used with the 12-bit resolution data acquisition system.

A thermal anemometer was used to measure the air velocity and the turbulence intensity. The average air velocities used in these experiments were 0.33, 0.70, 1.14 and 1.45 m/s. A series of calibration tests was conducted to determine the free stream velocity at five locations across the diameter of the pan and at six different elevations above the surface of the water. The maximum deviation was less than ±10% from the weighted average velocity. The overall average velocity was obtained by weighing the individual measurements by the chord length at the corresponding radial position. The turbulence intensity of the air stream was found to range between 0.05 and 0.08.

The evaporation wind tunnel experiment was placed in a cubical enclosure measuring 2.4 m on each side to isolate it from the rest of the laboratory. The enclosure had a computer controlled air conditioning system to maintain the inlet air of the wind tunnel at 20°C and 50% relative humidity.

2.1. Experimental procedure

Evaporation experiments were started by filling the water tank up to the rim so that the water surface was flush with the floor of the low speed wind tunnel. The inlet air was conditioned and the air stream in the wind tunnel was set at a fixed velocity during the warm up period until steady temperatures were achieved in the water basin. The basin was filled again up to the rim (usually requiring only a small amount of water compared to the total tank volume) and allowed to come back into thermal equilibrium again. The computer-based data acquisition system then recorded the air temperature and relative humidity and the water temperature based on the averages determined from the readings taken over 10-min intervals. The water mass change in the weighing pan over the 10-min interval was also recorded in the data file. The system was allowed to run for a 24-h period. The data analysis included averaging the measured quantities over the full measurement period to summarize the evaporation rate for the test run.

3. Results and discussion

It is appropriate to introduce the results in a form that directly shows the evaporation rate as a function of both the air velocity and the vapor pressure driving potential and to discuss the related error limits. These are shown in Fig. 2.

It is observed from the data that the evaporation rate for a fixed air velocity does not increase linearly with the vapor pressure differential. It has been observed by many investigators that with free convection evaporation, the vapor pressure driving potential carries an exponent usually of the order 1.2–1.3. Thus, it is evident that at low air velocities, a non-unity exponent on the vapor pressure differential is present. A regression analysis using a least squares fit on the data, yields a predictive model of the form:

$$J = a(P_w - P_a)^b, \tag{1}$$

where

$$a = 74.0 + 97.97V + 24.91V^2 \tag{2}$$

and

$$b = 1.22 - 0.19V + 0.038V^2. \tag{3}$$

In this expression the evaporation rate, J, is given in g/m^2 h, the air velocity, V, is in m/s and the vapor pressure terms, P_w and P_a, are in kPa.

A fixed error of ±7.5 g/m^2 h is present in the measured evaporation rate. This error is due to the uncertainties associated with the area of the evaporation surface, the proportionality constant for the weighing pan and the resolution of the electronic scale over a 24-h data collection period. The size of this error is less than the size of the data markers in Fig. 2 and is not shown.

The error in the vapor pressure driving potential is not a fixed value because vapor pressure is not a linear function of temperature. In general, the uncertainties in measuring the temperature and the relative humidity generated an error of ±0.1 kPa at 25°C water temperature. The error increased to ±0.16 kPa at 45°C. Error bars for these specific conditions are shown on the first and the penultimate data markers for the air velocity of 0.33 m/s in Fig. 2. In summary, the error on the vapor pressure is near the outside edges of the data markers.

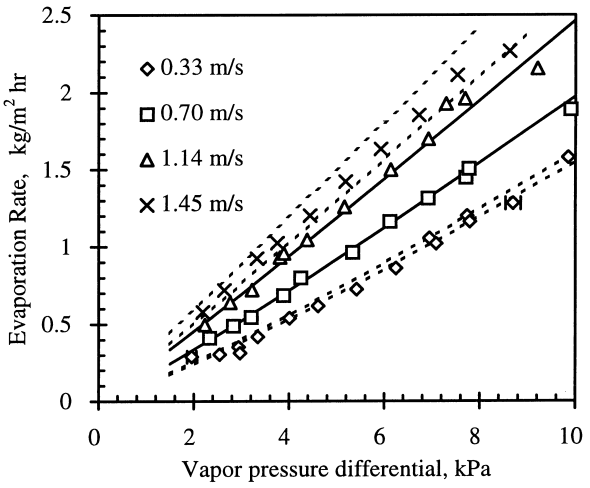

Fig. 2. Evaporation rate data at four air velocities.

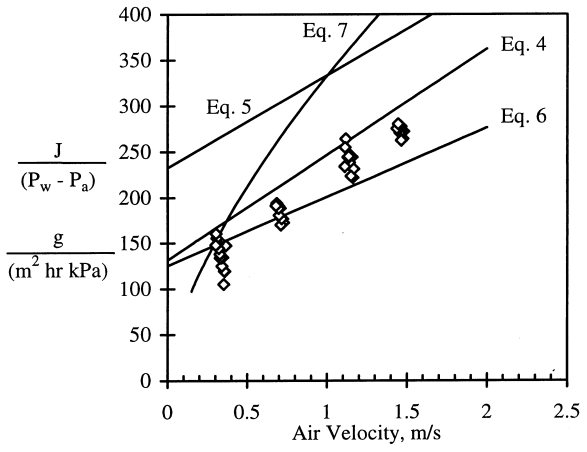

Fig. 3. Comparison of measured evaporation rate data with historical evaporation rate equations based on wind tunnel data.

The error in the wind speed of ±10% is shown as two dashed lines in Fig. 2 for the minimum and maximum air flow velocities. The nominal air velocities are shown by solid lines for the intermediate cases of 0.70 and 1.14 m/s. It is noted that all the data points lie within the error bounds described by the measured evaporation rate, the vapor pressure driving potential and the wind speed.

3.1. Comparison to wind tunnel-based evaporation models

Considerable variation exists in the predictions of available correlations for water evaporation into moving air currents. The differences in these correlations may be attributed to the nature, size and procedures used in the experiments. The trend among the predictions appears to be related to the pan size used in the experiments. Higher evaporation rates are predicted by smaller evaporation pans. Several historical predictive equations based on Dalton's model were compared to our data as shown in Fig. 3.

In 1918, Carrier [6] published his correlation for determining the evaporation rate. This equation is still used by engineers in the HVAC industry to determine the latent load requirements on air-conditioning systems that service natatoriums, spas and the like. Carrier did not describe the experimental apparatus or procedures used to obtain the data. Development of the evaporation rate correlation was of secondary importance in Carrier's effort to clarify the relation between wet-bulb and dry-bulb temperatures and vapor pressure differences for use in air-conditioning and drying applications. Hence, parameters relevant to evaporation rate measurements, other than air velocity, were not included in his paper. Carrier's equation is

$$J = 3370(95 + 83.7V)(P_w - P_a)/h_{fg}, \quad (4)$$

where h_{fg} is the enthalpy of vaporization of the water. This equation was found to be fairly accurate compared to our data, especially considering that Carrier's experiments used air velocities over the wide range 0–7.1 m/s. In general, the Carrier equation predicted evaporation rates about 15% higher than our observations.

Hinchley and Himus [7] published their results in 1924. Their experiments were conducted with relatively small pans having surface areas in the order 0.02–0.07 m^2. Although the water temperature, ambient conditions and wind speed were carefully maintained and monitored in a wind tunnel, their correlation predicts high evaporation rates. The edge effects caused by the small pan sizes may be one of the reasons for the large evaporation rates predicted by their correlation. Another reason may be the level of turbulence in their wind tunnel, which they specifically mention as a characterization of the air flow. It is not clear from their experimental apparatus description whether or not their fan acted as a blow-thru or a draw-thru unit. If their fan operated in the blow-thru mode, it could explain the high prediction of their correlation due to the highly turbulent conditions. Their correlation may be written as

$$J = (232.5 + 101V)(P_w - P_a). \quad (5)$$

The correlation of Rowher [5] predicts evaporation rates close to those observed by our experiments. Rowher used an evaporation pan (0.84 m^2) that was much larger than those of Hinchley and Himus. Rowher's correlation is

$$J = (125 + 75.5V)(P_w - P_a). \quad (6)$$

The prediction based on Powell's [8] work was based on experiments with a series of circular pans with a surface area ranging up to 0.20 m^2 and air velocities up to 10.0 m/s. Powell's relation, which is not valid for still air conditions, tends to over-predict the evaporation rate and is one of the few correlations that includes the pan diameter as a parameter. It may be written in the form by Powell as

$$J = 355(P_w - P_a)(Vd)^{0.65}/d, \quad (7)$$

where the pan diameter, d, is in meters.

3.2. Correlations based on dimensional analysis

Dimensional analysis on the evaporation process reveals that an equation for combined free and forced convection mass transfer is analogous to an equation describing heat transfer. The mass transfer coefficient, h_m, is defined by analogy to heat transfer as

$$J = h_m \rho (C_w - C_a), \tag{8}$$

where ρ is the density of the moist air mixture. The Sherwood number is used to define h_m as

$$\mathrm{Sh} = h_m L / D_{AB}, \tag{9}$$

where L is the characteristic length of the evaporation surface and D_{AB} is the binary diffusion coefficient of water vapor in air. Thus, the evaporation rate may be calculated from the Sherwood number using

$$J = (\mathrm{Sh}) D_{AB} \rho (C_w - C_a)/L. \tag{10}$$

In the mass transfer analogy the Sherwood number for evaporation in a moving air stream is given by the following nonlinear combination when the ratio $\mathrm{Gr}_m/\mathrm{Re}^2 \sim 1$

$$\mathrm{Sh} = [(\mathrm{Sh}_{free})^n + (\mathrm{Sh}_{forced})^n]^{(1/n)}. \tag{11}$$

For many mixed convective heat transfer problems the exponent n has a value between 3 and 4 when the Nusselt number is substituted in this equation for the Sherwood number [12]. However, based on evaporation correlations in the literature, it appears that the exponent n should have a value between 1 and 2 for mass transfer.

The Sherwood number must be defined for each evaporation regime. Thus for laminar free convection ($\mathrm{Gr}_m \mathrm{Sc} < 2 \times 10^7$) for an upward facing evaporation surface

$$\mathrm{Sh} = 0.54(\mathrm{Gr}_m \mathrm{Sc})^{1/4}, \tag{12}$$

where the mass transfer Grashof number is defined as

$$\mathrm{Gr}_m = \rho(\rho_a - \rho_i) g L^3 / \mu^2. \tag{13}$$

Here, ρ is the air density based on the average film temperature between the water and the ambient air. The free stream air density is ρ_a, the air density at the interface at 100% saturation is ρ_i and the dynamic viscosity of air is μ. The Schmidt number is defined by

$$\mathrm{Sc} = \mu/(\rho D_{AB}). \tag{14}$$

For turbulent free convection ($\mathrm{Gr}_m \mathrm{Sc} > 2 \times 10^7$) the Sherwood number is

$$\mathrm{Sh} = 0.14(\mathrm{Gr}_m \mathrm{Sc})^{1/3}. \tag{15}$$

For laminar forced convection ($\mathrm{Re}_L < 5 \times 10^5$) parallel to a rectangular evaporation surface, the mean Sherwood number over the length of the plate is found by

$$\mathrm{Sh} = 0.664 \mathrm{Sc}^{1/3} \mathrm{Re}_L^{1/2} \tag{16}$$

and for turbulent flow ($\mathrm{Re}_L > 5 \times 10^5$) over a rectangular plate with a laminar entrance region, the mean Sherwood number over the plate is

$$\mathrm{Sh} = \mathrm{Sc}^{1/3}(0.036 \mathrm{Re}_L^{0.8} - 836). \tag{17}$$

When the flow is turbulent over the entire evaporation surface due to tripping of the laminar boundary layer at the leading edge or by some other means of inducing turbulence, the appropriate form of the forced convection Sherwood number is:

$$\mathrm{Sh} = 0.036 \mathrm{Sc}^{1/3} \mathrm{Re}_L^{0.8}. \tag{18}$$

Since the boundary layer equations are developed for a rectangular plate of infinite width, a correction to the forced convection Sherwood number must be made to account for the circular geometry of the tested evaporation tank.

$$\mathrm{Sh}_{circ} = (\mathrm{Sh}) \frac{2}{\pi} \int_0^{\pi} \sin^{3/2} \theta \, d\theta, \tag{19}$$

where upon evaluating the integral: $\mathrm{Sh}_{circ} = 1.1128 \mathrm{Sh}$.

The Sherwood number for the data collected in these experiments was calculated using Eq. (10) based upon the observed evaporation rates. The free convection component of the Sherwood number was calculated from Eq. (15) since the evaporation took place under turbulent free conditions. The forced convection component was calculated using Eq. (18) (since the air flow had induced turbulence) with the modification of Eq. (19) to account for the circular evaporation surface. Fig. 4 shows the results of the Sherwood number calculations for the evaporation data using the ratio Sh(forced)/Sh(free) as the abscissa and the ratio Sh(total)/Sh(free) as the ordinate. Here Sh(total) = Sh(free) + Sh(forced). The calculated Sherwood numbers are shown as diamond markers and are plotted with Eq. (11) for values of $n = 1$, 2 and 3. The limiting cases

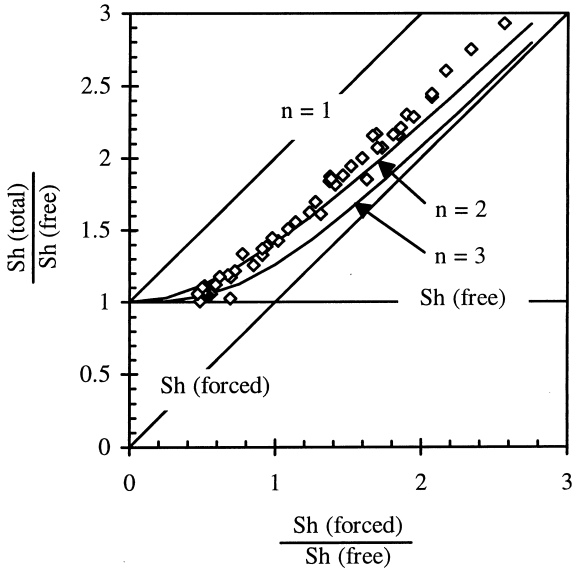

Fig. 4. Dependence of total evaporation rate on the ratio of forced to free convection with a comparison to predictions based on Eq. (11) for $n = 1$, 2, and 3.

of pure free convection and pure forced convection are also shown. This plot clearly shows that a quadratic combination (i.e. $n = 2$) of free and forced convection closely models the evaporation rate over a range in which neither component strongly dominates the other.

Dimensional analysis suggests that the combined effects of free and forced convection must be considered when the buoyancy and inertial forces are of the same order of magnitude. These forces are represented by the dimensionless product: Gr_m/Re^2. The experiments conducted in this investigation covered the range $0.1 < Gr_m/Re^2 < 10.0$. This not only includes the range in which combined convection modes are important, but also the limits where either free or forced convection effects might be neglected. A functional relationship between the evaporation rate and the forces that drive the evaporation process is desired. Such a correlation would be of the form: $Sh = f(Gr_m, Re, Sc)$. Fig. 4 shows that the forced convection component may be neglected until a threshold velocity is reached. This threshold velocity is dependent upon the temperature of the water, the air and the relative humidity. It may be calculated using the criteria of Sh(forced)/Sh(free) ≈ 0.5. Over the range Gr_m/Re^2 tested in our experiments it appears that the effect of the free convection cannot be neglected anywhere. An offset from pure forced convection is observed in the entire data set as shown in Fig. 4. This suggests a correlation of the form

$$Sh = Sh_{free}[1 + f(Gr_m/Re^2)], \tag{20}$$

in which the free convection Sherwood number is modified to include the effects of forced convection. The form of the f-function is shown in Fig. 5 with the evaporation data. This shows that for $Gr_m/Re^2 > 5.0$, the contribution of forced convection to the total evaporation rate is less than 10%. At the other extreme, it is noted that for $Gr_m/Re^2 = 0.1$, the free convection contribution to the evaporation rate is in the order of 30% and thus cannot be neglected. The least squares fit regression of the data shown in Fig. 5 describes the f-function as:

$$f = 0.543 - 0.408\left(\ln\left(\frac{Gr_m}{Re^2}\right)\right) + 0.0826\left(\ln\left(\frac{Gr_m}{Re^2}\right)\right)^2. \tag{21}$$

This equation is valid only over the range $0.1 < Gr_m/Re^2 < 10.0$.

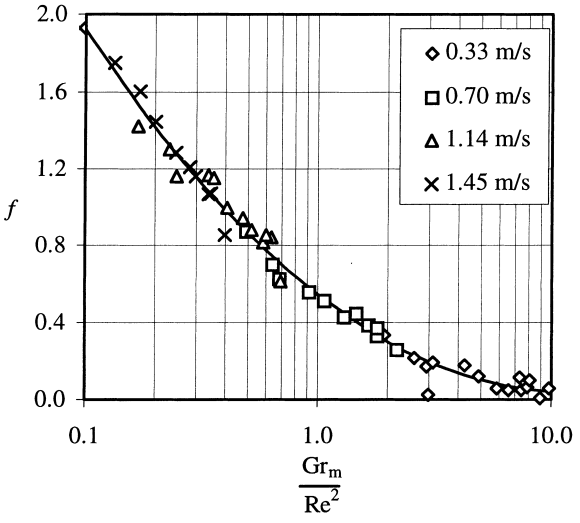

Fig. 5. Dimensionless f-function described by Eq. (21) correlated to the measured evaporation data.

4. Practical significance

Two systems of equations for predicting water evaporation into a moving air stream with a low velocity have been presented. Eqs. (1)–(3) provide a simple and accurate estimate of the evaporation rate in terms of the vapor pressure driving potential and the air velocity. The vapor pressure terms are easily determined from the knowledge of the water and air temperature and the air relative humidity using a table of properties of saturated water. This represents an improvement over the historical equations of Rowher, Carrier, Powell, and Hinchley and Himus, especially at low air velocities. These equations should be useful in providing more accurate estimates of evaporation from water surfaces that are indoors and are serviced by a forced air heating or cooling system.

A second system of equations, Eqs. (20) and (21), was also presented in dimensionless form. These are useful for extending the results to other surface geometries and air flow conditions. In these equations an appropriate form of the free convection Sherwood number such as Eq. (12) or Eq. (15) is used and modified to include the effects of forced convection. The characteristic dimension of the evaporating surface is included in the Grashof and the Reynolds numbers.

5. Future research needs

Evaporation of bulk fluids has been well researched over the last two centuries. Research in evaporation today focuses on the needs of specialty applications that are not adequately addressed by the presently available body of literature. Such special areas may range from evaporation losses from vented storage tanks to cooling hot surfaces with thin liquid films.

6. Conclusions

Measurements of the evaporation rate from a large diameter evaporation pan were made in a low speed wind tunnel. The air flow and water conditions allowed for examining the mixed mass convective effects over the range $0.1 < Gr_m/Re^2 < 10.0$. The data cover the range in which combined convection modes are important, as

well as the limits where either free or forced convection effects dominate.

The results were compared with several equations based on other experiments in the laboratory wind tunnels. Not all of the predictive equations proved to be accurate. The most accurate equations based on wind tunnel measurements were those of Carrier [6] and Rowher [5]. Since neither of these equations considers the non-linearity of the vapor pressure driving potential in the evaporation process, a new equation (Eq. (1)) was developed to account for this characteristic. This non-linearity has been observed in many free convection models.

A dimensional analysis was made to develop a functional relationship between the Sherwood number, the mass-based Grashof number, the Schmidt number and the Reynolds number. Examining the evaporation regime tested in these experiments revealed that forced convection effects are small or almost negligible when $Gr_m/Re^2 > 5.0$. However, free convection effects cannot be neglected over the range tested. It was found that at $Gr_m/Re^2 = 0.1$, 30% of the evaporation rate was contributed by the free convection component. A new correlation (Eqs. (20) and (21)) was developed to predict evaporation in mixed convection modes using the relation: $Sh = Sh_{free}[1 + f(Gr_m/Re^2)]$. For a 95% confidence level, the absolute percent deviation between the experimental and predicted Sherwood numbers is $\leqslant 7.9\%$. The correlation was developed for a Reynolds number range of 23,000 to 115,000 based on the evaporation surface diameter. However, it should be noted that the Reynolds number does not correspond to laminar flow conditions in these experiments. The air stream was intentionally made turbulent by tripping the boundary layer upstream of the evaporation surface. The mass-based Grashoff number (Eq. (13)) ranged from 1.2×10^9 to 5.5×10^9, while the Schmidt number (Eq. (14)) was essentially constant with a value of 0.61.

Nomenclature

C	molar concentration (kmol/m^3)
D_{AB}	binary mass diffusion coefficient (m/s)
Gr_m	mass transfer Grashof number (dimensionless, seeEq. (13))
J	evaporation rate (g/m^2 h)
L	characteristic length (m)
P	vapor pressure (kPa)
Re	Reynolds number (dimensionless)
Sc	Schmidt number (dimensionless, see Eq. (14))
Sh	Sherwood Number (dimensionless, see Eq. (9))
V	air velocity (m/s)
a	evaporation coefficient (see Eq. (2))
b	evaporation exponent (see Eq. (3))
d	pan diameter (m)
f	function describing forced component (see Eq. (21))
g	gravitational acceleration (m/s^2)
h_{fg}	enthalpy of vaporization (J/kg)
h_m	convective mass transfer coefficient (m/s)

Greek Symbols

ρ	density (kg/m^3)
μ	dynamic viscosity (kg/s m)

Subscripts

a	characteristic value in air
circ	based on circular surface area
free	free convection component
forced	forced convection component
L	based on characteristic length
i	characteristic value at the interface
total	sum of free and forced convection component
w	characteristic value in water

References

[1] J. Dalton, Experimental essays on the constitution of mixed gases; on the force of steam or vapor from water and other liquids in different temperatures, both in a Torricellian vacuum and in air; on evaporation and on the expansion of gases by heat, Memiors Manchester Lit. and Phil. Soc. 5 (1802) 535–602.

[2] E.M. Sparrow, G.K. Kratz, M.J. Schuerger, Evaporation of water from a horizontal surface by natural convection, J. Heat Trans. 105 (1983) 469–475.

[3] L.M.K. Boelter, H.S. Gordon, J.R. Griffin, Free evaporation into air of water from a free horizontal quiet surface, Indust. and Eng. Chem. 38 (1946) 596–600.

[4] M.T. Pauken, T.D. Tang, S.M. Jeter, S.I. Abdel-Khalik, A novel method for measuring water evaporation into still air, ASHRAE Trans. 99 (1) (1993) 297–300.

[5] C. Rowher, Evaporation from free water surface, US Deptartment of Agriculture in cooperation with Colorado Agricultural Experiment Station, Technical Bulletin no. 271, 1931.

[6] W.H. Carrier, The temperature of evaporation, ASHVE Trans. 24 (1918) 25–50.

[7] J.W. Hinchley, G.W. Himus, Evaporation in currents of air, J. Soc. Chem. Indust. 7 (1924) 57–63.

[8] R.W. Powell, Evaporation of water from saturated surfaces, Engineering 150 (1940) 238, 239; 278–280.

[9] B.A. Farley, An experimental investigation of the evaporation rate from stationary water pools into moving air, M.S. Thesis, G. W. Woodruff School of Mechanical Engineering, Georgia Institute of Technology, 1994.

[10] M.L. Albertson, La mécanique de l'évaporation (Mechanics of evaporation), La Houille Blanche 5 (1955) 704-717; 1 (1956) 39–52; 2 (1956) 285–311.

[11] M.T. Pauken, B. Farley, S.M. Jeter, S.I. Abdel-Khalik, An experimental investigation of water evaporation into low-velocity air currents, ASHRAE Trans. 101 (1) (1995) 90–96.

[12] F.P. Incropera, D.P. DeWitt, Fundamentals of Heat and Mass Transfer, 4th ed., Wiley, New York, 1996.